2014

HFO1234ze(Z) saturated vapour condensation inside a brazed plate heat exchanger

Giovanni A. Longo
University of Padova - DTG, Italy, tony@gest.unipd.it

Claudio Zilio
University of Padova - DTG, Italy, claudio.zilio@unipd.it

Giulia Righetti
University of Padova - DTG, Italy, giuliarighetti@gmail.com

J. Steven Brown
The Catholic University of America, US, brownjs@cua.edu

HFO1234ze(Z) Saturated Vapour Condensation inside a Brazed Plate Heat Exchanger

Giovanni A. LONGO[1*], Claudio ZILIO[1], Giulia RIGHETTI[1], J. Steven BROWN[2]

[1]University of Padova, Department of Management and Engineering
I-36100 Vicenza, Italy
tony@gest.unipd.it

[2]The Catholic University of America, School of Engineering
Washington DC, USA
brownjs@cua.edu

* Corresponding Author

ABSTRACT

This paper presents the experimental heat transfer coefficients and pressure drop measured during HFO1234ze(Z) saturated vapour condensation inside a small commercial BPHE: the effects of refrigerant mass flux and saturation temperature were investigated. The heat transfer coefficients show weak sensitivity to saturation temperature and great sensitivity to refrigerant mass flux. At low refrigerant mass flux (< 15 $kgm^{-2}s^{-1}$) the heat transfer coefficients are independent of mass flux and condensation is controlled by gravity. For higher refrigerant mass flux (> 15 kg $m^{-2}s^{-1}$) the heat transfer coefficients depend on mass flux and forced convection condensation occurs. The frictional pressure drop shows a linear dependence on the kinetic energy per unit volume of the refrigerant flow and therefore a quadratic dependence on the refrigerant mass flux. HFO1234ze(Z) shows heat transfer coefficients and frictional pressure drop higher than HFC236fa. The experimental results were compared against theoretical models for condensation heat transfer coefficients (Nusselt, 1916 and Akers *et al.*, 1959) and a new linear correlation for two-phase frictional pressure drop was presented.

1. INTRODUCTION

Although HFC refrigerants are estimated to account for less than 1% of the global warming effect of all greenhouse gases (Montzka, 2012), they will be subjected to a progressive phase-down or a more radical phase-out depending on international protocols or specific national or international legislation.

The low Global Warming Potential (GWP) alternatives to HFC refrigerants depend on application. Hydrocarbon refrigerants, such as HC600a (Isobutane) and R290 (Propane), have been already widely used in small domestic refrigerators and drink-coolers which require a reduced refrigerant charge and probably they are the more suitable low GWP substitute for HFC134a in this specific application. HFO1234yf refrigerant has been identified as a low GWP alternative to HFC134a in mobile air conditioning systems (Calm, 2008; Brown, 2009), whereas HFO1234ze(E) has been applied as drop-in replacement for HFC134a in large-capacity centrifugal chillers (Ueda *et al.*, 2012). Moreover HFO1234ze(E) and the isomer HFO1234ze(Z) are candidate substitutes for HFC236fa and HFC245fa in organic Rankine cycles and in high temperature heat pumps (Brown *at al.,* 2009, Fukuda *et al.,* 2014). In particular HFO1234ze(Z) exhibits a very high critical temperature, around 150°C, that allows operating sub-critical cycles at the high temperature required by industrial heat pumps. Therefore it seems to be the most promising low GWP refrigerant for high temperature heat pumps with potential capability similar to refrigerant CFC114 that had dominated this type of application before the Montreal Protocol.

In the open literature it is possible to find some experimental works on HFO1234yf (Del Col *et al.*, 2010; Park *et al.,* 2011; Wang *et al.,* 2012; Longo and Zilio, 2013) and HFO1234ze(E) (Park *et al.,* 2011b, Hossain *et al.,* 2012; Longo *et al.*, 2014) condensation, whereas data on HFO1234ze(Z) two-phase heat transfer is rather scarce.

This paper presents the experimental heat transfer coefficients and pressure drop measured during HFO1234ze(Z) saturated vapour condensation inside a small commercial BPHE: the effects of refrigerant mass flux and saturation temperature were investigated.

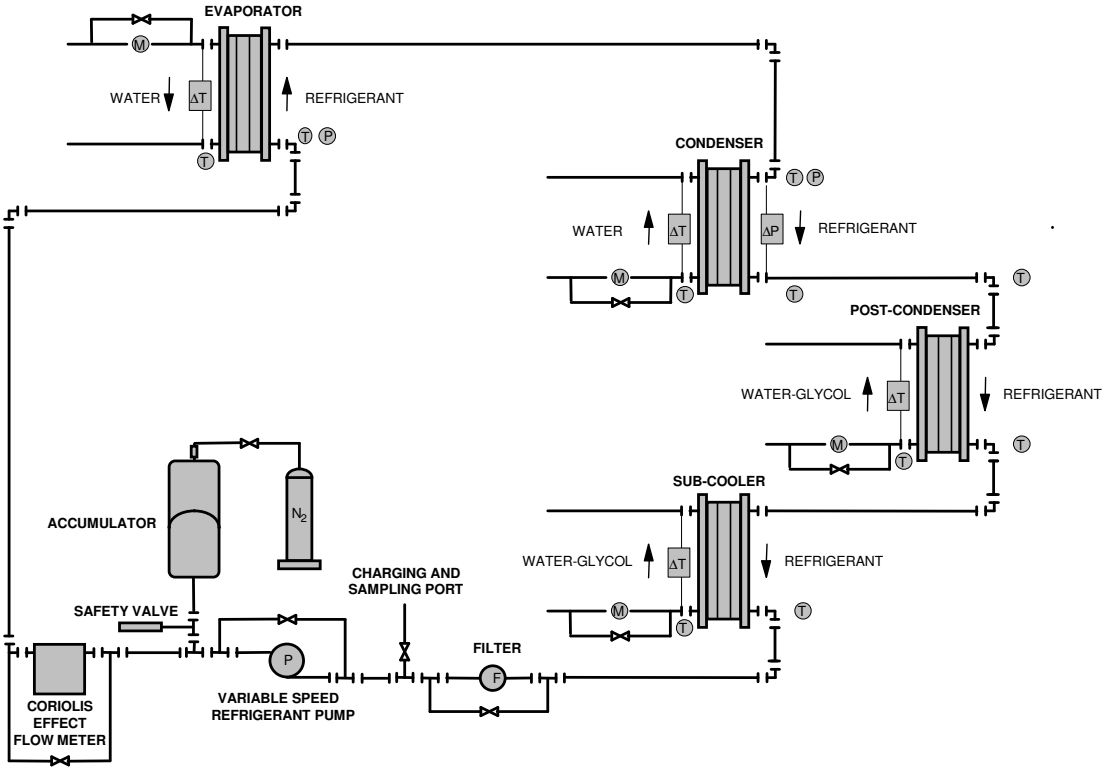

Figure 1: Schematic view of the experimental rig

2. EXPERIMENTAL SET-UP AND PROCEDURES

The experimental facility shown on figure 1 consists of a refrigerant loop, a water-glycol loop and two water loops. The condenser tested is a BPHE consisting of 10 plates, 72 mm in width and 310 mm in length, which present a macro-scale herringbone corrugation with an inclination angle of 65° and a corrugation amplitude of 2 mm. Figure 2 and table 1 give the main geometrical characteristics of the BPHE tested, whereas table 2 outlines the main features of the different measuring devices in the experimental rig. A detailed description of the experimental rig, the measurement devices and the operating procedures is reported by Longo (2010). The experimental results are reported in terms of refrigerant side heat transfer coefficients and frictional pressure drop.

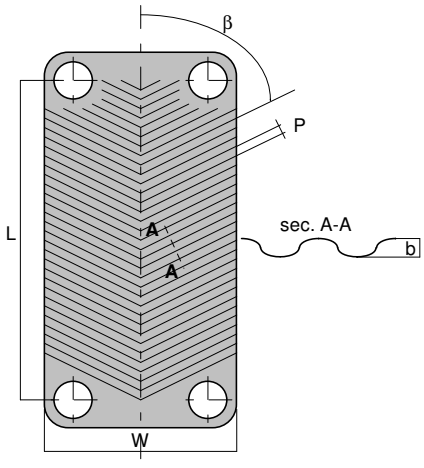

Figure 2: Schematic view of the plate

Table 1: Geometrical characteristics of the BPHE

Fluid flow plate length L(mm)	278.0
Plate width W(mm)	72.0
Area of the plate A(m^2)	0.02
Enlargement factor Φ	1.24
Corrugation type	Herringbone
Angle of the corrugation β(°)	65
Corrugation amplitude b(mm)	2.0
Corrugation pitch p(mm)	8.0
Number of plates	10
Number of effective plates N	8
Channels on refrigerant side	4
Channels on water side	5

Table 2: Specification of the different measuring devices

Device	**Type**	**Uncertainty (k= 2)**	***Range***
Thermometer	T-type thermocouple	0.1 K	-20 / 80°C
Differential thermometer	T-type thermopile	0.05 K	-20 / 80°C
Abs. pressure transducer	Strain-gage	0.075% f.s.	0 / 0.4 MPa
Diff. pressure transducer	Strain-gage	0.075% f.s.	0 / 0.3 MPa
Refrigerant flow meter	Coriolis effect	0.1% measured value	0 / 300 kg/h
Water flow meter	Magnetic	0.15% f.s.	100 / 1200 l/h

3. DATA REDUCTION

The overall heat transfer coefficient in the condenser U is equal to the ratio between the heat flow rate Q, the nominal heat transfer area S and the logarithmic mean temperature difference ΔT_{ln}

$$U = Q / (S \, \Delta T_{ln}) \tag{1}$$

The heat flow rate is derived from a thermal balance on the waterside of the condenser:

$$Q = m_w \, c_{pw} \, |\Delta T_w| \tag{2}$$

where m_w is the water mass flow rate, c_{pw} the water specific heat capacity and $|\Delta T_w|$ the absolute value of the water temperature lift across the condenser. The reference heat transfer area of the condenser

$$S = N \, A \tag{3}$$

is equal to the nominal projected area $A = L \times W$ of the single plate multiplied by the number N of the effective elements in heat transfer. The logarithmic mean temperature difference is equal to:

$$\Delta T_{ln} = (T_{wo} - T_{wi}) / \ln [(T_{sat} - T_{wi})/(T_{sat} - T_{wo})] \tag{4}$$

where T_{sat} is the average saturation temperature of the refrigerant computed from the measurement of refrigerant temperature at the inlet and at the outlet of the condenser, and T_{wi} and T_{wo} are the water temperatures measured at the inlet and the outlet of the condenser.
The average heat transfer coefficient on the refrigerant side of the condenser $h_{r.ave}$ is derived from the global heat transfer coefficient U assuming no fouling resistances:

$$h_{r.ave} = (1 / U - s / \lambda_p - 1 / h_w)^{-1} \tag{5}$$

by computing the water-side heat transfer coefficient h_w using a modified Wilson plot technique. A specific set of experimental water-to-water tests is carried out on the condenser to determine the calibration correlation for heat transfer on the water-side, in accordance with Muley and Manglik (1999): the detailed description of this procedure is reported by Longo and Gasparella (2007). The calibration correlation for water-side heat transfer coefficient is:

$$h_w = 0.277 \, (\lambda_w / d_h) \, Re_w^{0.766} \, Pr_w^{0.333} \tag{6}$$

$$5 < Pr_w < 10 \qquad 200 < Re_w < 1200$$

The refrigerant vapour quality at the condenser inlet and outlet X_{in} and X_{out} are computed starting from the refrigerant temperature $T_{e.in}$ and pressure $p_{e.in}$ measured at the inlet of the evaporator (sub-cooled liquid condition) considering the heat flow rate exchanged in the evaporator and in the condenser (Q_e and Q, respectively) and the pressures p_{in} and p_{out} measured at the inlet and outlet of the condenser as follows:

$$X_{in} = f(J_{in}, p_{in}) \quad (7)$$

$$X_{out} = f(J_{out}, p_{out}) \quad (8)$$

$$J_{in} = J_{e.in}(T_{e.in}, p_{e.in}) + Q_e / m_r \quad (9)$$

$$J_{out} = J_{in} - Q / m_r \quad (10)$$

$$Q_e = m_{e.w}\, c_{pw}\, |\Delta T_{e.w}| \quad (11)$$

where J is the specific enthalpy of the refrigerant, m_r the refrigerant mass flow rate, $m_{e.w}$ the water flow rate and $|\Delta T_{e.w}|$ the absolute value of the temperature variation on the waterside of the evaporator. The refrigerant properties are evaluated by Refprop 9.1 (NIST, 2013).
The frictional pressure drop on the refrigerant side Δp_f is computed by subtracting the manifolds and ports pressure drops Δp_c and adding the momentum pressure rise (deceleration) Δp_a and the gravity pressure rise (elevation) Δp_g to the total pressure drop measured Δp_t:

$$\Delta p_f = \Delta p_t - \Delta p_c + \Delta p_a + \Delta p_g \quad (12)$$

The momentum and gravity pressure drops are estimated by the homogeneous model for two-phase flow as follows:

$$\Delta p_a = G^2 (v_G - v_L)\, |\Delta X| \quad (13)$$

$$\Delta p_g = g\, \rho_m\, L \quad (14)$$

where v_L and v_G are the specific volume of liquid and vapour phase, $|\Delta X|$ is the absolute value of the vapour quality change between inlet and outlet and

$$\rho_m = [X_m / \rho_G + (1 - X_m) / \rho_L]^{-1} \quad (15)$$

is the average two-phase density between inlet and outlet calculated by the homogeneous model at the average vapour quality X_m between inlet and outlet. The manifold and port pressure drops are empirically estimated, in accordance with Shah and Focke (1998), as follows

$$\Delta p_c = 1.5\, G^2 / (2\, \rho_m) \quad (16)$$

4. ANALYSIS OF THE RESULTS

A set of 42 saturated vapour condensation data points with refrigerant HFO134ze(Z) down-flow and water up-flow was carried out at three different saturation temperatures: 30, 35 and 40°C. The inlet vapour quality varies between 0.91 and 0.97 and the outlet vapour quality between 0.00 and 0.06. Table 3 shows the experimental tests operating conditions: refrigerant saturation temperature T_{sat} and pressure p_{sat}, inlet and outlet refrigerant vapour quality X_{in} and X_{out}, refrigerant mass flux G_r and heat flux q. A detailed error analysis performed in accordance with Kline and McClintock (1954) indicates an overall uncertainty within ±12% for the refrigerant heat transfer coefficient measurement and within ±10 % for the refrigerant total pressure drop measurement.

Table 3: Operating conditions during experimental tests

Runs	$\mathbf{T_{sat}}$(°C)	$\mathbf{p_{sat}}$(MPa)	$\mathbf{X_{in}}$	$\mathbf{X_{out}}$	$\mathbf{G_r}$(kg m^{-2}s^{-1})	**q**(kW m^{-2})
42	29.9–40.1	0.21–0.30	0.91–0.97	0.0–0.06	7.7–33.0	5.1–23.3

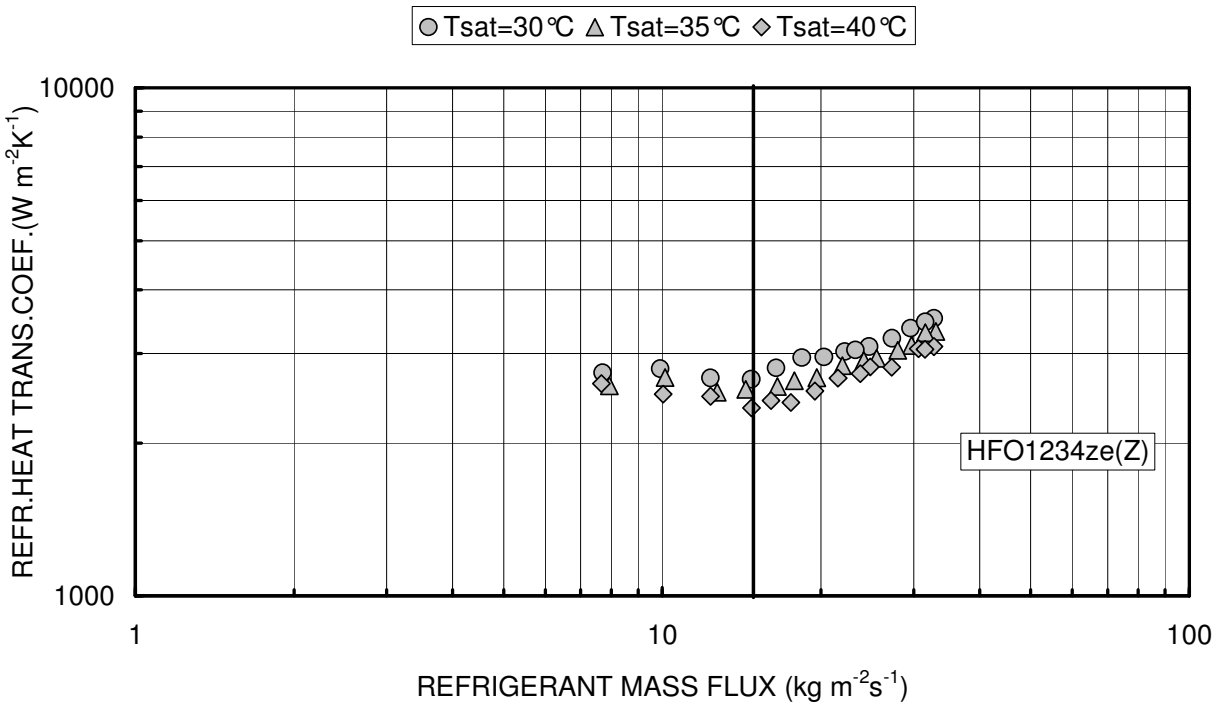

Figure 3: Average heat transfer coefficient on refrigerant side vs. refrigerant mass flux

Figure 3 shows the average heat transfer coefficients on the refrigerant side vs. refrigerant mass flux for saturated vapour condensation at different saturation temperatures (30, 35 and 40°C). The heat transfer coefficients show weak sensitivity to saturation temperature and great sensitivity to refrigerant mass flux. At low refrigerant mass flux (G_r < 15 kg $m^{-2}s^{-1}$) the heat transfer coefficients are not dependent on mass flux and probably condensation is controlled by gravity. For higher refrigerant mass flux (G_r > 15 kg $m^{-2}s^{-1}$) the heat transfer coefficients depend on mass flux and forced convection condensation occurs. In the forced convection condensation region a doubling of the refrigerant mass flux (from 15-16 to 30-33 kg $m^{-2}s^{-1}$) involves a 30% enhancement in the heat transfer coefficient (from 2500 to 3300 W $m^{-2}K^{-1}$). The heat transfer coefficients have been compared against the classical Nusselt (1916) analysis for laminar film condensation on vertical surface and the Akers *et al.* (1959) equation for forced convection condensation inside a tube. The Nusselt (1916) analysis is valid for gravity controlled laminar film condensation: the average heat transfer coefficient on the vertical surface results

$$h_{NUSSELT} = 0.943 \left[(\lambda_L^3 \rho_L^2 g \Delta J_{LG}) / (\mu_L \Delta T L)\right]^{1/4} \quad (17)$$

where ρ_L, λ_L and μ_L are the condensate density, thermal conductivity and dynamic viscosity respectively, ΔJ_{LG} is the specific enthalpy of vaporisation, g is the gravity acceleration, ΔT the difference between saturation and wall temperature and L the length of the vertical surface. This equation has been multiplied by the enlargement factor Φ (equal to the ratio between the actual area and the projected area of the plates) to compute the heat transfer coefficient inside the BPHE referred to the projected area of the plates

$$h_{r.ave} = \Phi \, h_{NUSSELT} \quad (18)$$

The enlargement factor Φ for the BPHE tested is equal to 1.24.
The Akers *et al.* (1959) equation developed for forced convection condensation inside tube results

$$h_{AKERS} = 5.03 (\lambda_L / d_h) Re_{eq}^{1/3} Pr_L^{1/3} \quad (19)$$

where

$$Re_{eq} = G\,[(1 - X) + X\,(\rho_L / \rho_G)^{1/2}]\,d_h / \mu_L \tag{20}$$

$$Pr_L = \mu_L\, c_{pL} / \lambda_L \tag{21}$$

are the equivalent Reynolds number and the Prandtl number respectively. This equation, valid for $Re_{eq} < 50000$, gives the local heat transfer coefficient which has been multiplied by the enlargement factor Φ and integrated by a finite difference approach along the heat transfer area to compute the average condensation heat transfer coefficient inside BPHE referred to the projected area of the plates

$$h_{r.ave} = (1 / S) \int_0^S \Phi\, h_{AKERS}\, dS \tag{22}$$

Figure 4a shows the comparison between the saturated vapour condensation heat transfer coefficients at low refrigerant mass flux ($G_r < 15$ kg $m^{-2}s^{-1}$) and the average heat transfer coefficients calculated by Nusselt (1916) (eq.18). Figure 4b shows the comparison between the saturated vapour condensation heat transfer coefficients at high refrigerant mass flux ($G_r > 20$ kg $m^{-2}s^{-1}$) and the average heat transfer coefficients calculated by Akers et al. (1959) (eq.22). The Nusselt (1916) equation reproduces the experimental data at low refrigerant mass flux with an absolute mean percentage deviation of 22.0%, whereas Akers *et al.* (1959) model predicts the experimental data at high refrigerant mass flux with an absolute mean percentage deviation of 10.4%.

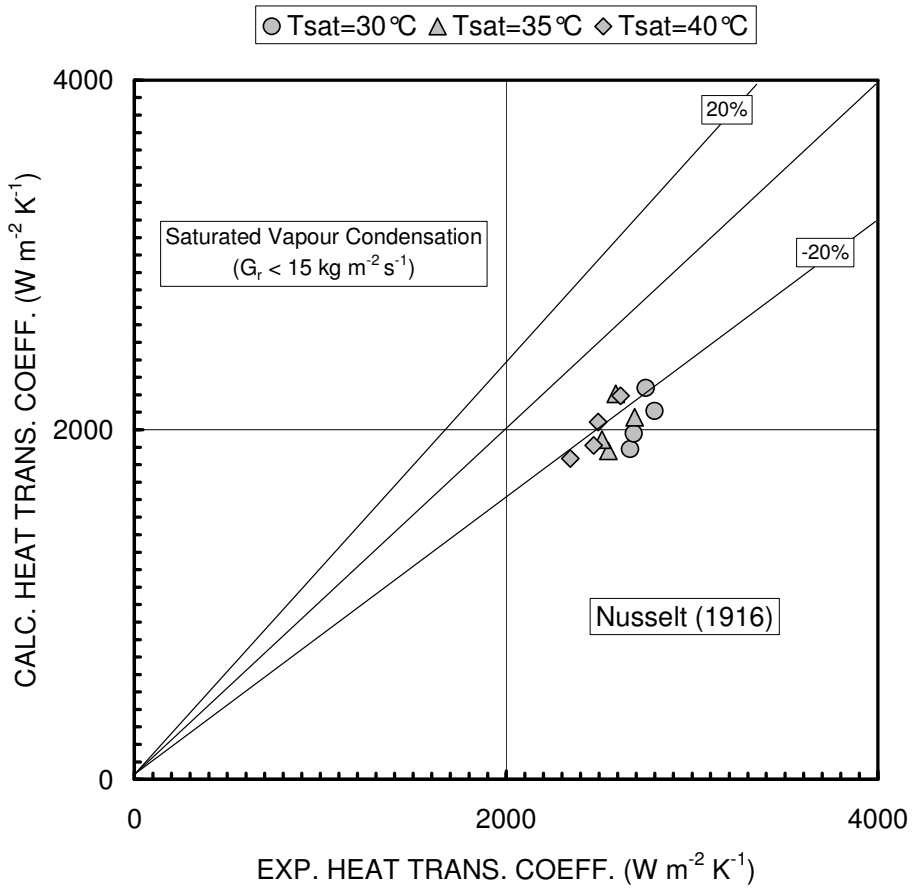

Figure 4a: Comparison between experimental and calculated heat transfer coefficients by Nusselt (1916) equation

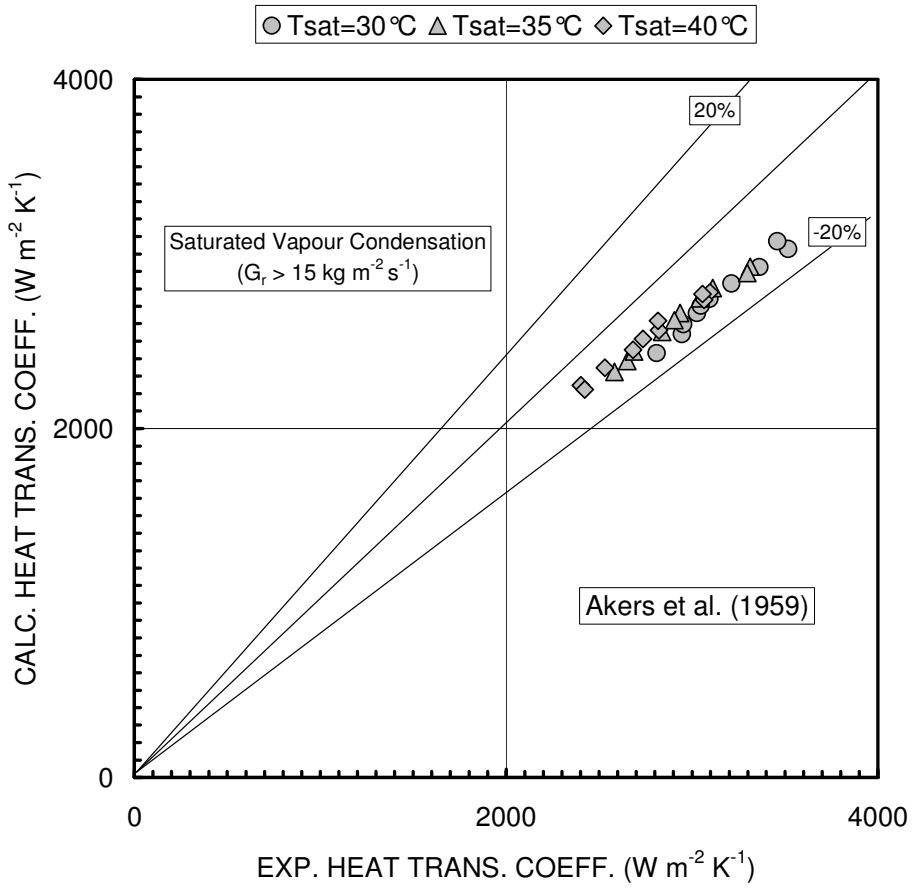

Figure 4b: Comparison between experimental and calculated heat transfer coefficients by Akers *et al.* (1959) model

Figure 5 shows the saturated vapour condensation frictional pressure drop against the kinetic energy per unit volume of the refrigerant flow computed by the homogeneous model:

$$KE/V = G^2/(2\,\rho_m) \tag{23}$$

The frictional pressure drop shows a linear dependence on the kinetic energy per unit volume of the refrigerant flow and therefore a quadratic dependence on the refrigerant mass flux. The following best fitting equation has been derived from present experimental data:

$$\Delta p_f = 1.8\ KE/V \tag{24}$$

This correlation reproduces present experimental data with a mean absolute percentage deviation around 7.7%.
HFO1234ze(Z) is a very promising substitute for HFC236fa in heat pump application and in organic Rankine cycles. Therefore it is interesting to compare the heat transfer and hydraulic performances of HFO1234ze(Z) refrigerant to those of HFC236fa. The present HFO1234ze(Z) condensation heat transfer coefficients and frictional pressure drop have been compared with those of HFC236fa previously measured by Longo (2010) inside the same BPHE under the same operating conditions. HFO1234ze(Z) exhibits higher heat transfer coefficients (48-82%) and frictional pressure drop (73-82%) than those of HFC236fa under the same operating conditions.

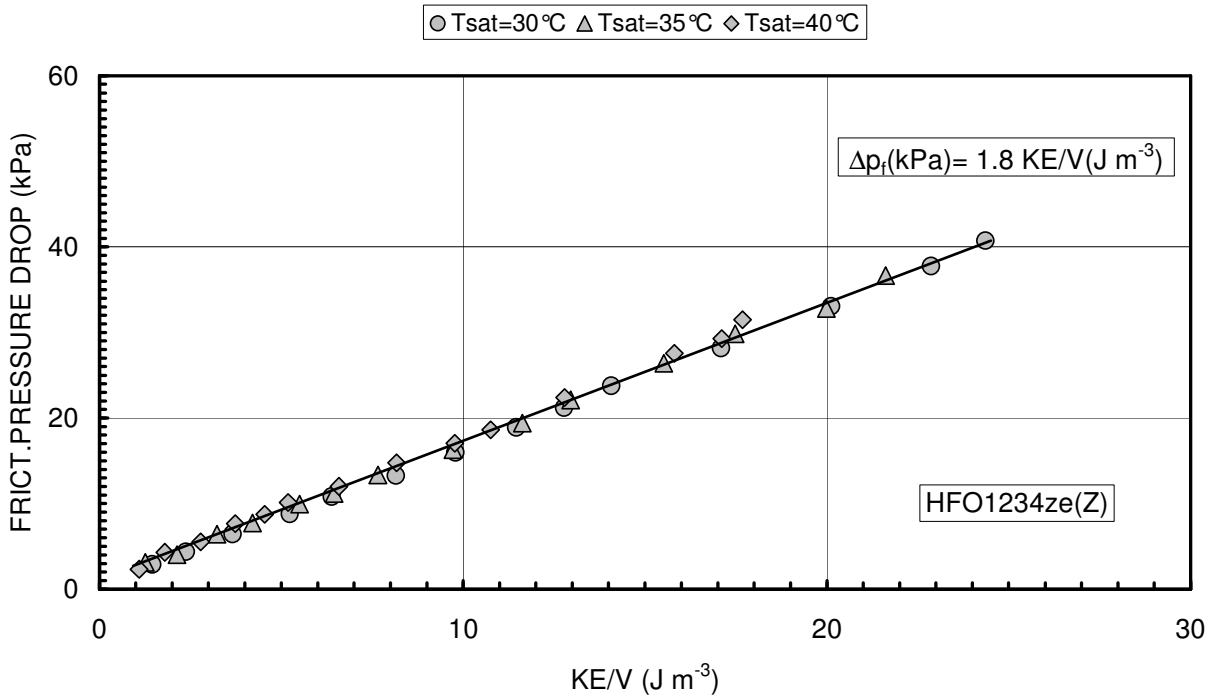

Figure 5: Frictional pressure drop vs. kinetic energy per unit volume

6. CONCLUSIONS

This paper investigates the effects of refrigerant mass flux and saturation temperature on heat transfer and pressure drop during HFO1234ze(Z) saturated vapour condensation inside a commercial BPHE. The heat transfer coefficients show weak sensitivity to saturation temperature and great sensitivity to refrigerant mass flux. The transition between gravity controlled and forced convection condensation occurs at a refrigerant mass flux around 15 kg $m^{-2}s^{-1}$. In the forced convection condensation region the heat transfer coefficients show a 30% enhancement for a doubling of the refrigerant mass flux. The frictional pressure drop shows a linear dependence on the kinetic energy per unit volume of the refrigerant flow and therefore a quadratic dependence on the refrigerant mass flux. The heat transfer coefficients are sufficiently well predicted by the Nusselt (1916) analysis for vertical surface in the gravity controlled region and by the Akers *et al.* (1959) model in the forced convection region. A linear equation based on the kinetic energy per unit volume of the refrigerant flow is proposed for the computation of frictional pressure drop. HFO1234ze(Z) exhibits higher heat transfer coefficients (48-82%) and frictional pressure drop (73-82%) than those of HFC236fa under the same operating conditions. Therefore it seems to be a very promising low GWP substitute for HFC236fa in high temperature heat pumps with a potential capability similar to refrigerant CFC114 that had dominated this type of application before the Montreal Protocol.

NOMENCLATURE

A	nominal area of a plate	(m^2)
b	height of the corrugation	(m)
c_p	specific heat capacity	(J $kg^{-1}K^{-1}$)
d_h	hydraulic diameter, $d_h = 2\ b$	(m)
f.s.	full scale	
g	gravity acceleration	(m s^{-2})
G	mass flux, $G = m / (n_{ch}\ W\ b)$	(kg $m^{-2}s^{-1}$)
h	heat transfer coefficient	(W $m^{-2}K^{-1}$)
J	specific enthalpy	(J kg^{-1})

k	coverage factor	
KE/V	kinetic energy per unit volume	(J m^{-3})
L	flow length of the plate	(m)
m	mass flow rate	(kg s^{-1})
N	number of effective plates	
n_{ch}	number of channels	
p	pressure	(Pa)
P	corrugation pitch	(m)
Pr	Prandtl number, Pr = $\mu c_p / \lambda$	
q	heat flux, $q = Q / S$	(W m^{-2})
Q	heat flow rate	(W)
Re	Reynolds number, Re = $G d_h / \mu$	
Re_{eq}	equivalent Reynolds number, $Re_{eq} = G [(1 - X) + X (\rho_L / \rho_G)^{1/2}] d_h / \mu_L$	
S	nominal heat transfer area	(m^2)
s	plate wall thickness	(m)
T	temperature	(K)
U	overall heat transfer coefficient	(Wm^{-2}K^{-1})
v	specific volume	(m^3 kg^{-1})
V	volume	(m^3)
W	width of the plate	(m)
X	vapour quality, $X = (J - J_L) / \Delta J_{LG}$	

Greek symbols

β	inclination angle of the corrugation	
Δ	difference	
ΔJ_{LG}	latent heat of vaporisation	(J kg^{-1})
ϕ	enlargement factor	
λ	thermal conductivity	(Wm^{-1}K^{-1})
μ	viscosity	(kg m^{-1}s^{-1})
ρ	density	(kg m^{-3})

Subscripts

a	momentum
ave	average
AKERS	Akers et al. (1959)
c	manifold and port
e	evaporator
eq	equivalent
f	frictional
g	gravity
G	vapour phase
in	inlet
L	liquid phase
LG	liquid gas phase change
ln	logarithmic
m	average value
NUSSELT	Nusselt (1916)
out	outlet
p	plate
pb	pre-evaporator
r	refrigerant
t	total
sat	saturation

REFERENCES

Akers, W.W., Deans, H.A., Crosser, O.K., 1959, Condensing heat transfer within horizontal tubes, *Chem. Eng. Prog. Symp. Series*, vol. 55, p. 171-176.

Brown, J.S., 2009, HFOs: new, low global warming potential refrigerants, *ASHRAE J.*, vol. 51, p. 22-29.

Brown, J.S., Zilio, C., Cavallini, A., 2009, The fluorinated olefin R-1234ze(Z) as a high-temperature heat pumping refrigerant, *Int. J. Refrig.*, vol. 32, p. 1412-1422.

Calm, J.M., 2008, The next generation of refrigerants d historical review, considerations, and outlook, *Int. J. Refrigeration*, vol. 31, p. 1123-1133.

Del Col, D., Torresin, D., Cavallini, A., 2010, Heat transfer and pressure drop during condensation of the low GWP refrigerant R1234yf, *Int. J. Refrig.*, vol. 33, p. 1307-1318.

Fukuda, S., Kondou, C., Takata, N., Koyama S., 2014, Low GWP refrigerants R1234ze(E) and R1234ze(Z) for high temperature heat pumps, *Int. J.Refrig.*, vol. 36, p. 161-173

Hossain, M.A., Onaka, Y., Miyara, A., 2012, Experimental study on condensation heat transfer and pressure drop in horizontal smooth tube for R1234ze(E), R32 and R410A, *Int. J. Refrigeration*, vol. 35, p. 927-938.

Kline, S.J., McClintock, F.A., 1954, Describing uncertainties in single-sample experiments, *Mech. Eng.*, vol. 75, p. 3-8.

Longo, G.A., Gasparella, A., 2007, Heat transfer and pressure drop during HFC refrigerant vaporisation inside a brazed plate heat exchanger, *Int. J. Heat Mass Transfer*, vol.50, p. 5194-5203.

Longo, G.A., 2010, Heat transfer and pressure drop during HFC refrigerant saturated vapour condensation inside a brazed plate heat exchanger, *Int. J.Heat Mass Transfer*, vol. 53, p. 1079-1087

Longo, G.A., Zilio, C., 2013, Condensation of the low GWP refrigerant HFO1234yf inside a brazed plate heat exchanger, *Int. J. Refrigeration*, vol. 36, p. 612-621.

Longo, G.A., Zilio, C., Righetti, G., Brown, J.S., 2014, Condensation of the low GWP refrigerant HFO1234ze(E) inside a Brazed Plate Heat Exchanger, *Int. J. Refrigeration*, vol. 38, p. *250-259*

Montzka, R., 2012, HFCs in the atmosphere: concentrations, emissions and impacts, Proc. of *ASHRAE/NIST* Conference, Gaithersburg, US

Muley, A., Manglik, R.M., 1999, Experimental study of turbulent flow heat transfer and pressure drop in a plate heat exchanger with chevron plates, *ASME J. Heat Transfer*, vol. 121, p. 110-121.

NIST, 2013, *Standard Reference Database, REFPROP 9.1.*

Nusselt, W., 1916, Die oberflachenkondensation des wasserdampfes, *Z. Ver. Dt Ing.*, vol. 60, p. 541-546, 569-575.

Park, K-J., Kang, D.G., Jung, D., 2011, Condensation heat transfer coefficients of R1234yf on plain, low fin, and Turbo-C tubes, *Int. J. Refrig.*, vol. 34, p. 317-321

Park, J.E., Vakili-Farahani, F., Consolini, L., Thome J.R., 2011b, Experimental study on condensation heat transfer in vertical minichannels for new refrigerant R1234ze(E) versus R134a and R236fa, *Exp. Therm. Fluid Sci.*, vol. 35, p. 442-454.

Shah, R.K., Focke, W.W., 1988, Plate heat exchangers and their design theory, *In*: Subbarao E.C., Mashelkar R.A., *Heat Transfer Equipment Design*, Hemisphere, Washington, p. 227-254.

Ueda, K., Hasegawa, Y., Wajima, K., Nitta, M., Kamada, Y., Yokoyama, A., 2012, Deployment of a new series of eco turbo ETI chillers, *Mitsubishi Heavy Industries Technical Review*, vol. 49, pp. 56-62.

Wang, L., Dang, C., Hihara, E. 2012, Experimental study on condensation heat transfer and pressure drop of low GWP refrigerant HFO1234yf in a horizontal tube, *Int.J.Refrig.*, vol. 35, p. 1418-1429

ACKNOWLEDGEMENT

This research project was partially funded by CariVerona Foundation, Verona, Italy, Ricerca Scientifica e Tecnologica, Sviluppo di innovativi processi a ridotto impatto ambientale per la conservazione e distribuzione a bassa temperatura delle derrate alimentari a salvaguardia della salute, 2013-2014.

The authors would like to thank also Central Glass Co. Ltd. for donating the refrigerant sample.